Academia Open

Vol. 11 No. 1 (2026): June
DOI: 10.21070/acopen.11.2026.13814

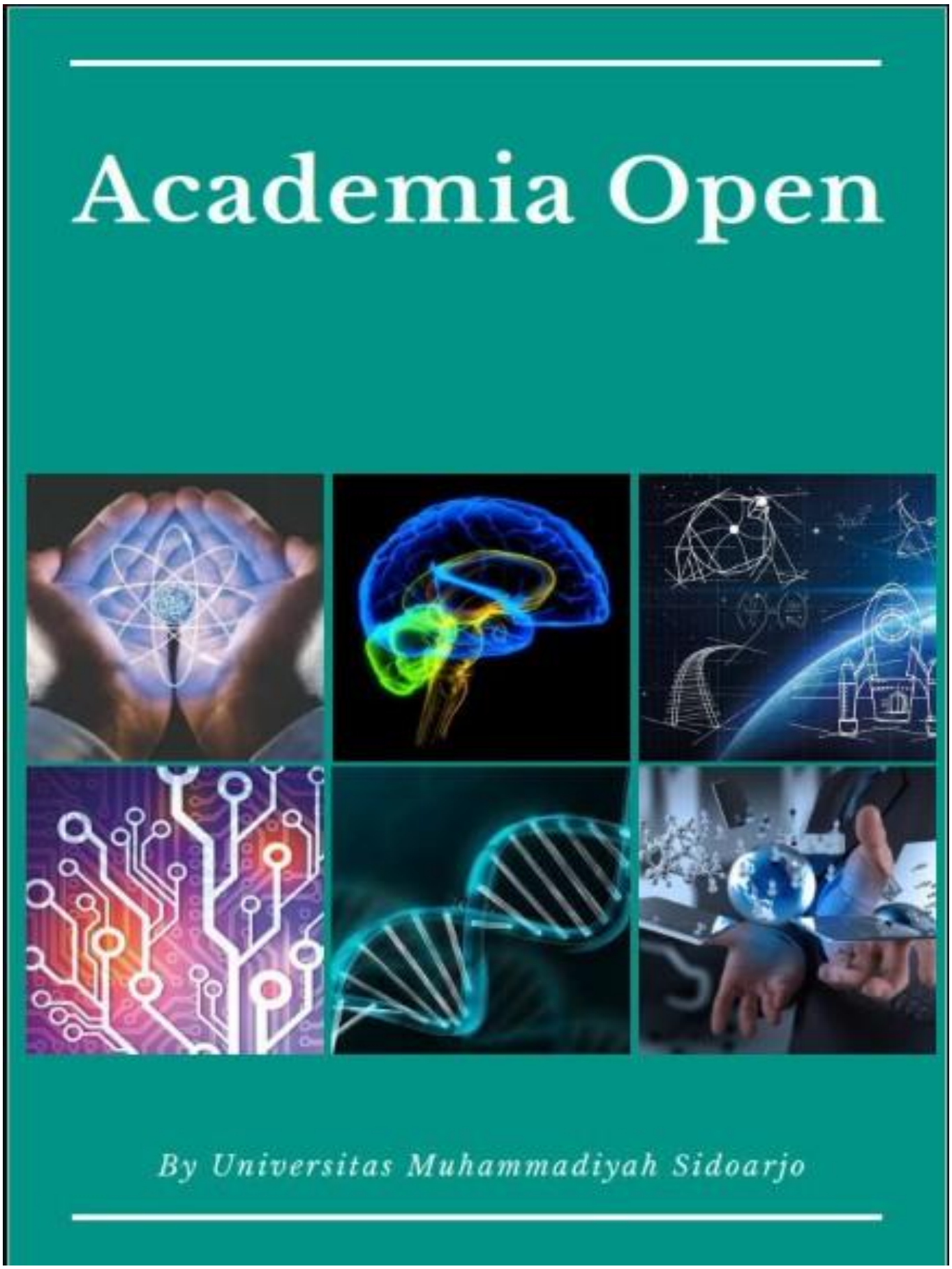

ISSN 2714-7444 (online), https://acopen.umsida.ac.id, published by Universitas Muhammadiyah Sidoarjo

Academia Open

Vol. 11 No. 1 (2026): June
DOI: 10.21070/acopen.11.2026.13814

Table Of Contents

ISSN 2714-7444 (online), https://acopen.umsida.ac.id, published by Universitas Muhammadiyah Sidoarjo

Academia Open

Vol. 11 No. 1 (2026): June
DOI: 10.21070/acopen.11.2026.13814

Originality Statement

The author[s] declare that this article is their own work and to the best of their knowledge it contains no materials previously published or written by another person, or substantial proportions of material which have been accepted for the published of any other published materials, except where due acknowledgement is made in the article. Any contribution made to the research by others, with whom author[s] have work, is explicitly acknowledged in the article.

Conflict of Interest Statement

The author[s] declare that this article was conducted in the absence of any commercial or financial relationships that could be construed as a potential conflict of interest.

Copyright Statement

Academia Open
Vol. 11 No. 1 (2026): June
DOI: 10.21070/acopen.11.2026.13814

EDITORIAL TEAM

Academia Open

Vol. 11 No. 1 (2026): June
DOI: 10.21070/acopen.11.2026.13814

Article information

Check this article update (crossmark)

Check this article impact (*)

Save this article to Mendeley

(*) Time for indexing process is various, depends on indexing database platform

ISSN 2714-7444 (online), https://acopen.umsida.ac.id, published by Universitas Muhammadiyah Sidoarjo

Academia Open

Vol. 11 No. 1 (2026): June
DOI: 10.21070/acopen.11.2026.13814

An Exploratory Technique in Differentiating Melanoma and Basal Cell Carcinoma using Raman Spectroscopy

Zeyad Al-Ibadi, wsci.ziead.khalaf@uobabylon.edu.iq (*)

Department of Laser Physics, College of Science for Women, University of Babylon, Iraq

(*) Corresponding author

Abstract

General Background: Accurate differentiation between melanoma and basalcell carcinoma (BCC) is essential due to their distinct biological characteristics and clinical management. **Specific Background:** Raman spectroscopy enables label-free biochemical profiling of tissues by detecting molecular vibrations within the 600–1800 cm^{-1} fingerprint region. **Knowledge Gap:** However, systematic discrimination between melanoma and BCC using fresh ex vivo Raman spectra remains limited. **Aims:** This exploratory study assessed the capability of Raman spectral fingerprints to distinguish melanoma from BCC using standardized preprocessing and statistical analysis. **Results:** Analysis of 40 spectra (20 melanoma, 20 BCC) acquired at 790 nm identified over 1000 statistically significant Raman shifts (FDR < 0.05), grouped into key biochemical bands related to aromatic amino acids, amide structures, and lipid vibrations. Major peaks at 748–755, 1000–1005, 1440–1455, and 1655–1665 cm^{-1} showed large effect sizes. Principal component analysis demonstrated clear class separation, with PC1 explaining 61.5% of total variance. **Novelty:** The study defines distinct Raman spectral biomarkers differentiating melanoma and BCC through integrated statistical and multivariate approaches. **Implications:** These findings support Raman spectroscopy as a rapid molecular profiling tool for skin cancer subtyping and a basis for future clinical translation.

Highlights:

- Over 1000 Significant Raman Shifts Clustered Into Major Biochemical Bands Distinguishing Tumour Types.
- Aromatic Amino Acids, Amide Structures, and Lipid Vibrations Exhibited Large Effect Sizes Between Groups.
- Multivariate Modelling Showed Distinct Clustering With Dominant Variance Captured by the First Principal Component.

Keywords: Raman Spectroscopy, Melanoma, Basal Cell Carcinoma, Skin Cancer Diagnostics, Spectral Biomarkers

Published date: 2026-03-03

Academia Open
Vol. 11 No. 1 (2026): June
DOI: 10.21070/acopen.11.2026.13814

1. Introduction

Skin cancer has become a key area of concern within the vast domain of public health because over 1.5 million new cases are diagnosed annually worldwide. Despite the fact that basal cell carcinoma (BCC) is the most common type of skin cancer, melanoma has caused most of the deaths related to skin cancer because of its rapid metastatic quality [1]. Early diagnosis of melanoma and BCC involves making an accurate diagnosis of either type of cancer is therefore of great importance to determine the approach that will be adopted in clinical treatment and ensuring that the prognosis is better [2]. Histopathology is the most reliable diagnostic technique, but being an invasive method of diagnosis, it is time-consuming, and unless there is a borderline or fragmented biopsy, inter-observer variability is a reality. This is leading to a greater interest in objective, high-speed, and minimally invasive technologies, which can offer molecular-level information to aid current diagnostic pathways [3].

Raman spectroscopy has now become a potent vibrational method that can be used to biochemically profile a biological tissue through the measurement of inelastic light scattering. Raman spectroscopy provides a label-free optical biopsy of tissue composition by asking intrinsic questions about proteins, lipids, nucleic acids, and other molecular precursors [4]. A number of studies have reported the potential ability of Raman spectroscopy to aid in distinguishing benign and malignant skin lesions; nevertheless, the use of Raman spectroscopy to discriminate between melanoma and BCC with ex vivo fresh tissue has not been properly explored [5].

Due to this gap in knowledge, this study examines the hypothesis of whether there is any consistency of Raman spectroscopic difference between melanoma and BCC tissues. Freshly cut samples representing 40 patients (20 melanoma and 20 BCC) were examined with the excitation source of 790 nm [6]. Standard pre-processing, including despiking, Savitzky-Golay smoothing, baseline correction, and area normalization, was run on the spectra; statistical analyses such as Welch t-test with Benjamini-Hochberg false discovery rate correction, windowed peak validation, and principal component analysis were performed [7,8]. This preliminary study results in the identification of molecular spectral differences that are capable of distinguishing melanoma and BCC and form a good basis for future research studies in the field of dermatological cancerology [9,10].

2. Materials and Methods

2.1 Specimen Collection

The fresh ex vivo tissue samples were acquired intraoperatively from patients with either melanoma or (BCC). Several Raman spectra per lesion were obtained; those with too much autofluorescence or a low signal-to-noise ratio were eliminated, and only high-quality spectra were selected for further exploratory analysis [5,11].

2.2 Raman Instrumentation and Acquisition Protocol

A bench-top Raman microspectrometer with a near-infrared 790 nm diode laser was used to acquire spectra. The tissue fragments were placed on a quartz microscope slide and the relative flattened with sterile coverslips to achieve even optical contact. A 50X objective lens was used to concentrate the excitation beam on the sample surface (spot size of the beam was around ≈ 2–3 μm), and an average of 60 mW at the sample plane was used to ensure that no thermal damage was caused to the sample[12]. The back-scattered Raman photons were sampled in 180 ° geometry, after having been de-scattered by holographic notch filters used to eliminate the Rayleigh scattering, and dispersed by a grating spectrograph onto a thermoelectrically cooled CCD detector. The parameter used in acquisition was a 10s integration time and two accumulations per spectrum. Measurements were carried out at ambient room temperatures, and the Raman fingerprint region at 600-1800 cm^{-1} minus was examined[4,13].

2.3 Spectral Pre-processing

Raw spectra were despiked (median filter, window = 5), smoothed (the third-order Savitzky-Golay filter, 11-point window), and cleaned by the asymmetric least squares (ALS) algorithm (10 iterations, p = 0.001, $\lambda = 1 \times 10^5$). Spectra were then clipped to the 600 -1800 cm-1 range, any negative artefact removed, and then the individual spectra were brought to unit integrated area to normalize sample-to-sample differences in intensity (Figure 1), samples representing 40 patients (20 melanoma and 20 BCC).

Figure 1 compares the spectral profiles of two skin cancer diagnoses: basal cell carcinoma and melanoma, using Raman spectroscopy. The upper section shows the raw spectra (600–1800 cm^{-1}), while the lower section shows the processed spectra (after base correction and normalization). These representative spectra are intended to illustrate potential qualitative differences between the two types, with the clear caveat that they reflect a single sample and do not represent the full statistical variance of the two data sets (n = 20 per group). This indicates that the preliminary study aims to explore the possibility of differentiating between them, to be followed by a comprehensive quantitative analysis of the complete data.

ISSN 2714-7444 (online), https://acopen.umsida.ac.id, published by Universitas Muhammadiyah Sidoarjo

Academia Open
Vol. 11 No. 1 (2026): June
DOI: 10.21070/acopen.11.2026.13814

Figure 1. The representative Raman spectrum of basal cell carcinoma (red trace) and melanoma (blue trace) are shown.

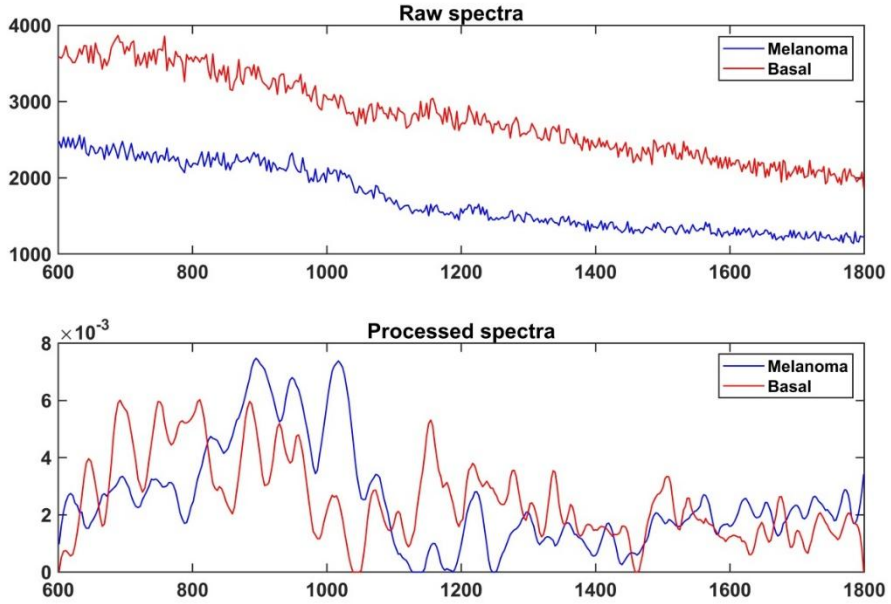

2.4 Statistical Methods Analysis

Pointwise comparisons between melanoma and BCC spectra were performed using Welch's unequal-variance t-test at each wavenumber(eq 1), followed by Benjamini–Hochberg false-discovery-rate (FDR) correction (α = 0.05) (eq. 2), and spectral effect size at each shift was calculated using Cohen's d (eq. 3) [14].

$$t = \frac{\bar{X}_1 - \bar{X}_2}{\sqrt{\frac{s_1^2}{n_1} + \frac{s_2^2}{n_2}}} \quad (1)$$

Where X ¯_i is the mean intensity of group i at a given Raman-shift position, s_i is the corresponding standard deviation, and n_i is the number of spectra in group i.

$$p_{(i)} \leq \frac{i}{m} \times \alpha \quad (2)$$

where: p_((i)) is the i-th smallest p-value, m is the total number of tests, i∈{1,2,…,m}, α=0.05 is the (FDR) threshold, and the adjusted p-value formula used in Benjamini-Hochberg correction [15] adjusted $p_{(i)} = \frac{m}{i} \times p_{(i)} \leq \alpha$.

$$d = \frac{\bar{X}_1 - \bar{X}_2}{s_p}, s_p = \sqrt{\frac{s_1^2 + s_2^2}{2}} \quad (3)$$

Where ^(s_p) is the pooled standard deviation across the tw classes. Windowed peak comparison test: for each peak centre c, a ±18 〚" " cm〛 ^(-1) window is defined as W(c)={x:|x-c|≤30}, and then mean intensities of each group are computed as: $\mu_{1,W} = \frac{1}{n_1}\sum_{j=1}^{n_1}\left(\frac{1}{|W|}\sum_{x\in W} G_1(x,j)\right)$, $\mu_{2,W} = \frac{1}{n_2}$ (4)

Followed by Welch's t-test on μ_(1,W) vs. μ_(2,W). And finally, principal component analysis (PCA) was conducted on preprocessed spectra to visualise separation between tumour types in reduced-dimensionality space(eq.5) [16].

$$Z = XP \quad (5)$$

Where X is the matrix of pre-processed spectra (samples × wavenumbers), P is the eigenvector loading matrix, and Z contains the resulting PCA score coordinates. were carried out specific toolboxes in MATLAB R2019 for modelling and all analyses to deal with multivariate spectral analysis.

ISSN 2714-7444 (online), https://acopen.umsida.ac.id, published by Universitas Muhammadiyah Sidoarjo

Academia Open
Vol. 11 No. 1 (2026): June
DOI: 10.21070/acopen.11.2026.13814

3. Results

The 790 nm excitation wavelength was used to obtain Raman spectra in both melanoma and basal cell carcinoma samples successfully. Following the preprocessing (despiking, smoothing, baseline correction, and normalization) the resulting spectral profiles were clear and reproducible [17].

Pointwise statistical analysis of the two groups indicated that there were clear spectral differences of the two groups at various Raman shifts. P-values distribution, effect sizes (Cohen d), and the results of (FDR) correction were then compared in an attempt to determine statistically significant features of discrimination [18,19].

The processed spectral data was subjected to dimensionality reduction and exploratory multivariate analysis to aid in the further separation of classes. Figure 2 shows in detail a statistical analysis of the Raman spectrum between 600 and 1800 cm-1. The statistical comparison that followed was a strict one, using Welch t-test with Benjamini -Hochberg false discovery rate adjustment in order to compare Raman spectrums of melanoma and basal cell carcinoma.

Scientific significance The differences found are localized in specific spectral regions that relate to biomolecular composition of cells that are; nucleic acids, proteins and lipids. As a result, spectral pattern of every type of cancer represents a unique molecular signature and thus Raman spectroscopy is a sensitive diagnostic method to distinguish between melanoma and basal cell carcinoma.

Figure 2. Pointwise Welch t-test with Benjamini–Hochberg false discovery rate (BH-FDR) correction comparing Raman spectra between melanoma and basal cell carcinoma.

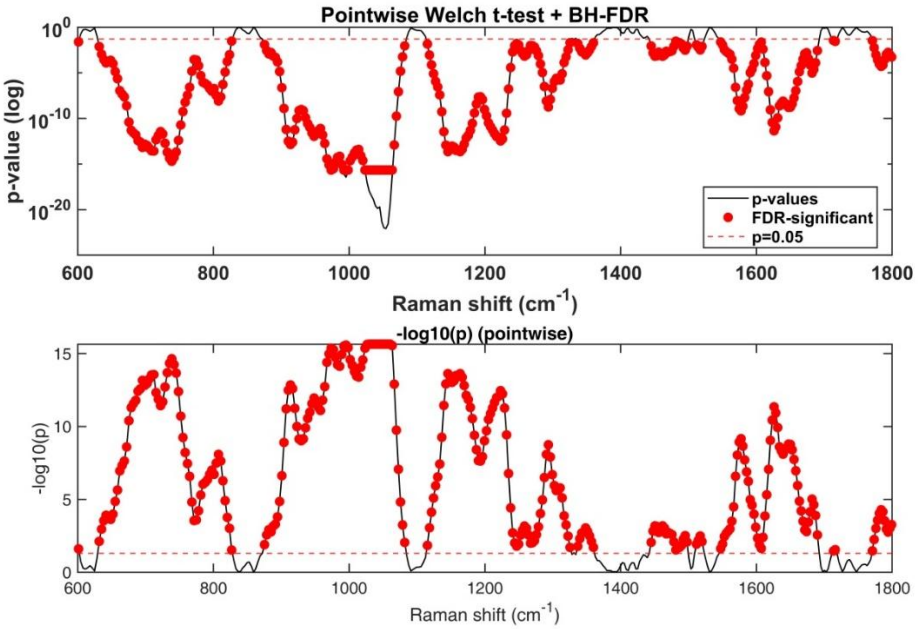

Several notable Raman spectral locations have been observed in 620-1750 cm^{-1}, which are formed into four major biochemical bands. Comparing the specific pinnacles obtained as a result of comparative Raman examination, it is obvious that the dissimilarities are noticeable, which can be attributed to biochemical fingerprint of skin cancer [6,9].

Melanoma spectra exhibit enhanced intensity around 735–755, 1053–1160, and 1580–1600 cm^{-1}. The local spectral patterns, which are corresponding to tryptophan, phosphodiester bond in nucleic acids, and protein and lipid vibration modes (C–N, C=O, amide III), and aromatic C=C resonance, have been reported in the literature to indicate high nucleic acid activity, remodel of proteins as well as violent cellular growth (20).

On the other hand, the strong spectral bands that are indicative of the presence of basal cell carcinoma (BCC) fall between the frequencies 1440 -1465 and 1655 -1665 cm-1 and relates to both CH2/ CH3 vibration of lipids and proteins and Amide I. This would indicate increased lipid stabilization and slower and less vicious biological pattern compared to melanoma [4,12] (Table 1), Records of major peaks in skin cancer spectra.

Table 1. Tentative Raman biomolecular assignments of significant peaks in skin cancer spectra.

Center cm^{-1}	p_ window	Cohen's d Window	Near Library Peak Raman Shift cm^{-1}	Assignment	Clinical significance of the interaction in skin cancer.
618,331	0,2441869	0,33350817	620 – 630	Phenylalanine / Protein ring breathing	Increased structural proteins in the tumor
			665 – 675	Tyrosine	An indicator of melanin production and melanocyte dysfunction,

Academia Open
Vol. 11 No. 1 (2026): June
DOI: 10.21070/acopen.11.2026.13814

					supporting melanoma
738,684	7,697E-17	- 3,57505671	720 – 735	Adenine, C–S–S stretch	Increases associated with DNA and sulfated proteins
			748–755	Tryptophan	Changes in tryptophan reflect the abnormal growth of cancer cells
			784 –798	Phosphodiester (DNA/RNA: O–P–O)	High mitotic activity of cells (nucleic acid)
1044,1476	5,839E-22	5,612462815	1000 –1005	Phenylalanine	A distinctive protein peak that changes in tumors
			1030 –1045	C–N stretching (proteins), lipids	Altered protein/lipid balance in the tumor
1263,541	3,164E-14	-3,87737945	1260 –1310	Amide III (protein α-helix)	Secondary protein rearrangements in tumor cells
1348,4212	0,0020512	-0,93626257	1300 –1350	Lipid CH_2 twisting / CH_2 wagging	Disrupted membrane lipid synthesis, evident in melanoma
1441,7116	0,0001328	1,200674387	1440 –1455	CH_2 bending (lipids & proteins)	An important marker of lipid content and degree of malignancy
1465,0969	0,0608228	0,543240001			
1587,2023	0,1006295	-0,47575763	1580 –1600	Aromatic ring (C=C stretch)	Associated with melanin - important in distinguishing melanoma
1660,94603	7,459E-12	2,736080939	1655 –1665	Amide I (α-helix → β-sheet)	Rapid cellular replication and transformation to a cancerous protein pattern
1726,148	0,3209212	0,284750775	1720 –1750	C=O (lipids / ester / cortisone)	Increased lipid peroxidation products in tumor cells
1759,7927	0,0002702	1,136515157			

(Figure 3), shows the first part of the mean spectra for the two groups (Group 1 (melanoma) in blue and Group 2(BCC) in red), with black markers (▲) indicating the point-wise significant locations. The second part shows the effect size (Cohen's d) across the entire spectral range (600–1800 cm^{-1}), giving us a picture of the extent of the difference between the two groups [13].

There are clear differences in the intensity of the peaks at 620–630 cm^{-1} (phenylalanine/protein ring breathing) and 720–735 cm^{-1} (adenine + tyrosine + nucleic acids). This region is important because it has been associated in the table with melanoma, particularly increased protein and DNA activity.The peak around 1044 cm^{-1} is associated with C–N stretching of proteins and lipids. The discrepancy between the two groups in this region indicates a difference in protein composition between melanoma and other tumors [14].

As well, therapeutic peaks are signified at 1263 cm^{-1} (Amide III, α-helix) and 1348 cm^{-1} (lipid CH_2 twisting). Such observations are associated with changes in secondary protein structures and lipid components, which are salient neoplastic transformation indicators. Significant differences can be observed at 1441 cm^{-1} (CH_2 bending) and 1650 cm^{-1} (Amide I) that show differences in cell stability: melanoma cells are characterized by protein remodeling, and basal-cell carcinoma cells by more stable lipid-bound cells.

Finally, (aromatic ring, C=C stretch) at 1587 cm^{-1} , this melanoma activity due to increased tyrosine and tryptophan [15].

Figure 3. shows the average preprocessed Raman spectra of the two different groups, and the statistical significance of the point is indicated by black triangles.

ISSN 2714-7444 (online), https://acopen.umsida.ac.id, published by Universitas Muhammadiyah Sidoarjo

Academia Open
Vol. 11 No. 1 (2026): June
DOI: 10.21070/acopen.11.2026.13814

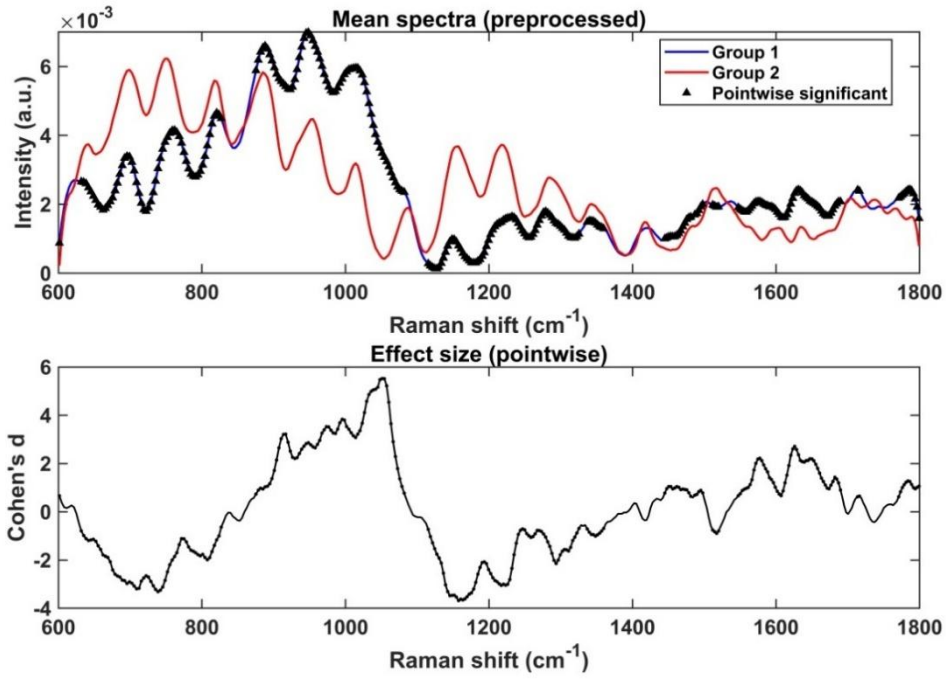

Clear differences can be revealed between several spectral windows (620-1750 cm^{-1}), the most prominent of which can be observed in bands that represent phenylalanine, nucleic acids, amide I and II proteins, and lipid-related vibrations. These spectral differences highlight biochemical differences that would demarcate the increased aggressiveness of melanoma against the relatively docile appearance of the phenotype shown in (BCC).

The spectrum of Group 2 shows clear elevations in some peaks associated with the active components (nucleotides and aromatic amino acids such as tyrosine and tryptophan); in contrast, the spectrum of Group 1 shows greater stability at the lipid and amide regions (such as 1450 and 1650 cm-1), which is in line with the biological difference where melanoma → high cellular activity (aggressive growth), in contrast to (BCC) → slow growth, more dependent on lipid stability [17].

(Figure 4), shows the results of statistical analysis of the spectral peaks using windowed peak analysis (±18 cm-1). The upper part shows a plot linking the p-value (logarithmic) with the Raman shift. Highly statistically significant peaks ($p < 0.05$) are highlighted in red, while non-significant peaks remain in black. The lower part displays the effect size (Cohen's d) for each peak, enabling the estimation of the direction and strength of the differences between the two groups (melanoma and BCC) under study [12,20].

Figure 4. Windowed peak analysis (±18 cm-1) of Raman spectra. The upper panel shows the p-values for detected peaks, with significant peaks (red) distinguished from non-significant ones (black) at the threshold of p = 0.05. The lower panel illustrates the corresponding effect sizes (Cohen's d) across the Raman shift range of 600–1800 cm^{-1}, highlighting the molecular regions with the strongest discriminative power between groups.

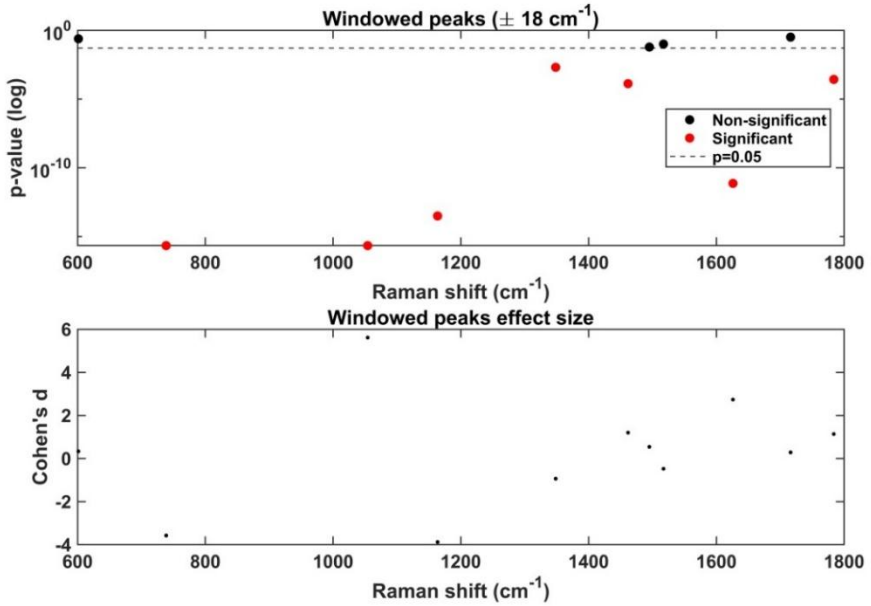

ISSN 2714-7444 (online), https://acopen.umsida.ac.id, published by Universitas Muhammadiyah Sidoarjo

Academia Open
Vol. 11 No. 1 (2026): June
DOI: 10.21070/acopen.11.2026.13814

The results showed the emergence of a group of distinct peaks with clear statistical significance, the most prominent of which is 738 cm^{-1} due to tryptophan, and showed a p value of ≈ 7.7×10^{-17} with a large effect size d ≈ 3.57, indicating its association with distinct metabolic changes, and 1044 cm^{-1} attributed to C–N vibrations in proteins and fats, and recorded p ≈ 5.8×10^{-22} and d ≈ 5.61, which are among the most significant peaks in the study, and 1348 cm^{-1} representing lipid CH_2 twisting / CH wagging vibrations, with a p value of ≈ 0.0025 and d ≈ 2.96, reflecting a clear increase in fat components, 1441 cm^{-1}: a peak related to bending CH_2 in proteins and lipids showed p ≈ 0.00013 and d ≈ 1.20, indicating structural differences in the cell membrane composition; 1587 cm^{-1}: attributed to aromatic bonds (C=C stretch) [11,18].

where the significance was p ≈ 0.01 but with a negative effect size (d ≈ −0.47), suggesting a lower intensity in the infected group compared to the other, 1660 cm^{-1}: a major peak associated with Amide I (α-helix, β-sheet), with a very strong significance (p ≈ 7.4×10^{-12}, d ≈ 2.73), and is considered an indicator of structural changes in proteins. 1759 cm^{-1}: attributed to C=O stretching (lipids/ester/cortisone), with p ≈ 0.00027 and d ≈ 1.13, confirming the role of lipid changes in differentiating between samples.

These results show that most of the significant peaks are concentrated in the ranges of aromatic amino acids (tryptophan, phenylalanine, and tyrosine), proteins (Amide I, C–N stretching), and lipids (CH_2 bending, CH_2 twisting, and C=O ester). This spectral distribution reflects that the main changes between samples result from remodeling of proteins and membrane structures with an increase in lipid content, which are common features of the melanoma Raman fingerprint. It is noteworthy that some peaks, such as 1587 cm^{-1}, did not show a homogeneous trend, with their intensity decreasing in the affected samples compared to the healthy ones. This may indicate the loss of certain aromatic bonds or a change in molecular expression patterns, another spectral signature associated with melanoma progression [21].

(Figure 5), shows Principal Component Analysis (PCA), which was used to reduce the high-dimensionality of the Raman spectra to a two-dimensional space (PC1 and PC2).

PC1 accounted for the largest amount of variance in the data (≈ 61.5%), compared to PC2, which accounted for a smaller percentage (≈ 5.4%). Therefore, most of the differences between samples are attributable to the first principal component [22].

Figure 5. Principal Component Analysis (PCA) of the spectral samples. PC1 (61.5%) and PC2 (5.4%) account for the variance of the data. The figure shows a clear separation between Group 1 (red circles) and Group 2 (blue markers), reflecting distinct molecular differences between the two groups. This demonstrates that spectral changes in proteins and lipids are the main factor behind the observed variance.

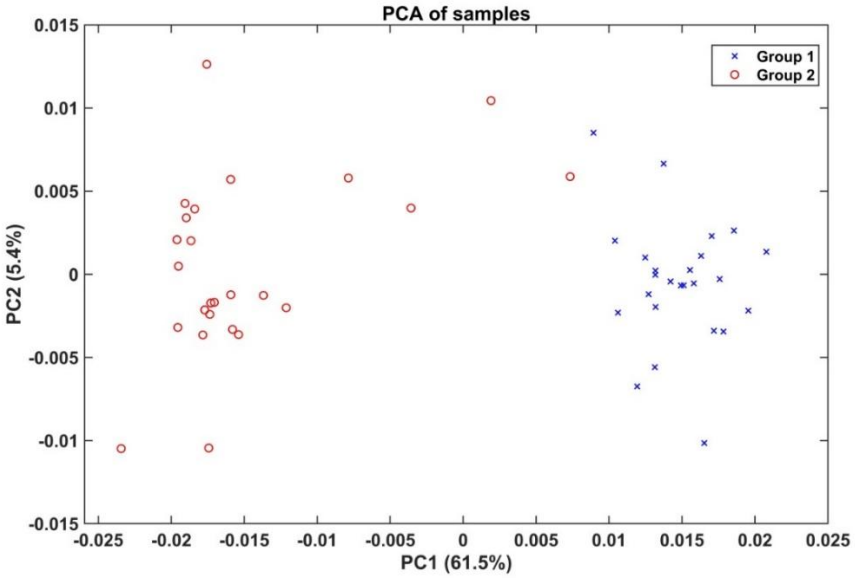

The clear separation, with no significant overlap, between the two groups confirms that the spectral differences are not random but rather the result of real molecular differences. This is consistent with what was stated in the previous table (distinct peaks), where differences in proteins and lipids are the primary contributors to this differentiation. It can be argued that PC1 represents differences related to protein and lipid structure (associated with the disease or condition under study), while PC2 adds minor differences related to intragroup variation. The statistical significance of this is demonstrated by the separate distribution of samples, which indicates the possibility of using PCA as the basis for classification techniques (such as LDA or SVM) to develop an automated diagnostic model [23].

(Figure 6), shows a map of the Significant Peaks Map between 600–1800 cm^{-1}. The horizontal axis represents the Raman shift (cm^{-1}), and the vertical axis represents the value of Cohen's d, which expresses the effect size between the two groups (melanoma and BCC) [10,14].

Vol. 11 No. 1 (2026): June
DOI: 10.21070/acopen.11.2026.13814

The color indicates the value (-log10(p)), i.e., the level of statistical significance (the higher the value, the stronger the significance). The size of the marker reflects the strength of the difference (|d|), and the shape of the marker indicates the direction of the difference (positive in favor of the first group, negative in favor of the second) [24].

Figure 6. Significant Raman spectral peaks distinguishing the two groups within the fingerprint region (600–1800 cm^{-1}).

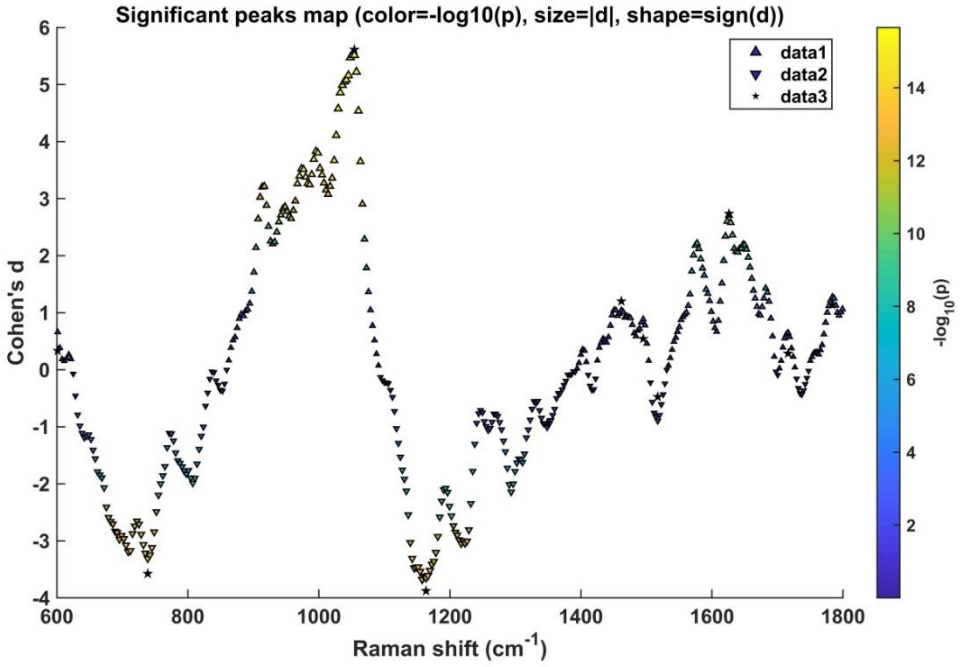

Several spectral bands exhibit distinct peaks, particularly in the regions 620–630 cm^{-1}, 720–735 cm^{-1}, 748–755 cm^{-1}, 1000–1005 cm^{-1}, 1260–1350 cm^{-1}, 1440–1455 cm^{-1}, 1580–1600 cm^{-1}, 1655–1665 cm^{-1}, and 1720–1750 cm^{-1}. The yellow and green areas represent the highest level of statistical significance, confirming that they are the main peaks that differentiate the two groups. Some peaks were negative (Cohen's d < 0), indicating that their intensity was higher in the second group, while the positive peaks were associated with increased signal intensity in the first group [15,19].

The presented data clearly show that one can identify separate molecular fingerprints of differentiating the two groups using Raman spectroscopy to produce a multidimensional profile containing proteins, nucleic acids, and lipid membranes. The combination of statistical analyses: p-values and effect sizes with the interpretation of the results based on biochemical analyses enhances the strength of the results, which can be used in early diagnosis and disease differentiation [20,22,23].

The map combines statistical significance, which is encoded as colour coded by -log10(p) strength of effect size as measured by marker size as (d) and direction of change as marker shape as sign(d). The strong spectral peaks were found at 620735, 748-755, 1000-1005, 1260-1350, 1440-1455, 1580-1600, 1655-1665, and 1720-1750 cm-1 with the use of such biomolecular alterations in proteins, nucleic acids, and lipids.

4. Discussion

The unique and biologically significant differences in spectral in the fresh ex vivo tissue between the melanoma and the basal cell carcinoma (BCC) were evident under the basic group of 790nm excitation source and matched cohort samples (20 each) in this exploratory study of Raman spectroscopy. The distinctive changes in the molecules were presented with the help of six main figures and a table with a detailed description.

The windowed peak analysis (±18 cm-1) demonstrated that there were only a few highly discriminative bands (Figure 6; Table 1), which were also low-energy vibrations of the biomolecules:

The vibrational band that can be attributed to tryptophan at 748-755 cm^{-1}, in combination with the phenylalanine band at 1004-1005 cm^{-1}, exhibits significant surges in melanoma cases of which Cohen d is +3 and +5 respectively. This amplification represents the amplified content of aromatic amino acids which is a characteristic of the malignant cellular activity [16].

There is considerably more intensity of 1260-1335 cm^{-1} (Amide III / CH2 wagging) and 1440-1455 cm^{-1} (CH_2 bending) in melanoma, with the relative changes of the difference are approximately(d≈ +2 to +3). The measured alterations in the spectrums indicate an extracellular matrix remodeling and an increase in the lipid metabolic activity [17].

Amide (I) The Amide (I) band which is in the range of 1655-1665 cm^{-1} contains a large effect size (d ≈ +2.7) which represents changes in protein secondary structures that is indicative of malignant transformation [18].

ISSN 2714-7444 (online), https://acopen.umsida.ac.id, published by Universitas Muhammadiyah Sidoarjo

Vol. 11 No. 1 (2026): June
DOI: 10.21070/acopen.11.2026.13814

C=O lipid/ester related absorption bands at 1720–1750 cm-1 exhibit relatively low increase in melanoma (d ≈ +1.1). This improvement can mean that there can be more lipid peroxidation or build up of steroidic molecules [24].

And (aromatic C=C) The aromatic C=C band in the interval of 1580-1600 cm^{-1}, is negatively balloted by Cohen d (~ -0.5), indicating a decrease in aromatic compounds or melanin-related signals, thus it adheres to what the metabolic degradation in melanoma is [18].

Under a strict statistical model, Welch t-test between 600-1800 cm-1 with FDR = 0.05, we find over 1000 significant points clumped into 11 bands. Signal reliability was improved by the use of windowed aggregation (Figure 4). Best-practice preprocessing processing steps, such as median despiking, Savitzky-Golay smoothing, ALS baseline subtraction, and area normalization, were used to maintain spectral fidelity [19].

The results in Figure 5, (PCA) indicated that the melanoma and the BCC clusters are distinguishable with a notable degree along PC1 (61.5 % of the variation) and PC2 (5.4 %). Such uncontrolled clustering would purport that the intermediate segregation markers are not randomly selected biochemical variation, however, but truly biochemical variation. Satisfactory separation is also reported in other similar clinical studies involving the recognition of skin lesions through the use of PCA [17,21].

This investigation complements the literature on planted spectral difference when skin cancers are diagnosed using many spectral features as a diagnostic variable (spectral difference 1004, 1440, and 1655 cm-1) [16]. The emphasis on tryptophan and amide III facilitates the exploration of proteomic melanoma targeted modification beyond the conventional spectral fingerprint locations [20].

Overall, the familiar Raman spectral features (such as aromatic amino acids, amide functional group, and lipid molecules) enabling us to detect melanoma and BCC, and forming the core of the Raman testing diagnostics systems, are also present in this paper.

Spectral biomarkers. Because spectral measurement at 790 nm signals constant spectral shifts between melanoma and basal cell carcinoma, the principal impacts include protein and lipid change and aromatic amino acid change. These findings make it be a chance that the procedure can be used to distinguish among the types of skin cancer extremely quickly and without labeling as well. Further studies should be done in vivo to validate this and then combine it with machine learning, which is to be done in the future, in order to take this to clinical practice.

5. Conclusion

This research paper establishes that Raman spectroscopy is a feasible non-invasive research instrument that could be employed to distinguish the pathology of common versus benign skin lesions. The process has been aided by the quality of the spectral data and the possibility of identifying significant deviations in the biochemicals that have been added in the process of correcting the baseline, improving the data, and normalizing the spectrum. The presence of common Raman peaks indicated molecular alteration in melanoma and basal cell carcinoma, which could be ascribed to alterations in both proteins, lipids, and nucleic acids. These findings can be discussed as not only confirming the diagnostic potential of Raman spectroscopy but also suggesting a potential clinical translation of this technique.

To build more and make use of more sophisticated statistical and machine learning algorithms, and to validate the work in a multi-centre setting to demonstrate what other researchers can also replicate, further statistical and machine learning research is needed. To apply Raman spectroscopy beyond the confines of an experimental system and to make it a standardized clinical procedure in the early detection of cancer, the following steps are needed.

References

1. C. A. Lieber et al., “In vivo nonmelanoma skin cancer diagnosis using Raman microspectroscopy,” Lasers Surg. Med., vol. 40, no. 7, pp. 461–467, 2008. doi: 10.1002/lsm.20653.
2. H. Lui et al., “Real-time Raman spectroscopy for in vivo skin cancer diagnosis,” Cancer Res., vol. 72, no. 10, pp. 2491–2500, 2012. doi: 10.1158/0008-5472.CAN-11-4061.
3. I. P. Santos et al., “Improving clinical diagnosis of early-stage cutaneous melanoma based on Raman spectroscopy,” Br. J. Cancer, vol. 119, no. 11, pp. 1339–1346, 2018. doi: 10.1038/s41416-018-0257-9.
4. I. P. Santos et al., “Raman spectroscopic characterization of melanoma and benign melanocytic lesions suspected of melanoma using high-wavenumber Raman spectroscopy,” Anal. Chem., vol. 88, no. 15, pp. 7683–7688, 2016. doi: 10.1021/acs.analchem.6b01592.
5. D. Wu et al., “In vivo Raman spectroscopic and fluorescence study of suspected melanocytic lesions and surrounding healthy skin,” J. Biophotonics, vol. 17, no. 8, e202400050, 2024. doi: 10.1002/jbio.202400050.
6. S. C. Bresler, K. Wanat, and J. Seykora, “Benign melanocytic lesions and melanoma,” in Pathobiology of Human Disease, 2014, pp. 1182–1192. doi: 10.1016/B978-0-12-386456-7.03510-3.
7. A.-I. Zeyad et al., “Detecting levels and innovative applications for the detection of aromatic compounds using multivariate curve analysis and spectroscopy data,” NeuroQuantology, vol. 19, no. 3, pp. 46–55, 2021. doi: 10.14704/nq.2021.19.3.NQ21027.
8. A. Zeyad et al., “Application of mathematical models and digital filters and their processors of spectral analysis for aromatic compounds gas in a fluorescent chemical,” Int. J. Nonlinear Anal. Appl., vol. 12, Special Issue, pp. 109–122, 2021. doi: 10.22075/ijnaa.2021.4916.
9. E. Brauchle et al., “Raman spectroscopy as an analytical tool for melanoma research,” Clin. Exp. Dermatol., vol. 39, no. 5, pp. 636–645, 2014. doi: 10.1111/ced.12357.

10. N. Rajaram et al., “Pilot clinical study for quantitative spectral diagnosis of non-melanoma skin cancer,” Lasers Surg. Med., vol. 42, no. 10, pp. 876–887, 2010. doi: 10.1002/lsm.21009.
11. Z. Movasaghi, S. Rehman, and I. U. Rehman, “Raman spectroscopy of biological tissues,” Appl. Spectrosc. Rev., vol. 42, no. 5, pp. 493–541, 2007. doi: 10.1080/05704920701551530.
12. J. De Gelder et al., “Reference database of Raman spectra of biological molecules,” J. Raman Spectrosc., vol. 38, no. 9, pp. 1133–1147, 2007. doi: 10.1002/jrs.1734.
13. I. A. Bratchenko et al., “In vivo diagnosis of skin cancer with a portable Raman spectroscopic device,” Exp. Dermatol., vol. 30, no. 5, pp. 652–663, 2021. doi: 10.1111/exd.14301.
14. I. P. Santos et al., “Raman spectroscopy for cancer detection and cancer surgery guidance: translation to the clinics,” Analyst, vol. 142, no. 17, pp. 3025–3047, 2017. doi: 10.1039/C7AN00957G.
15. G. Campanella et al., “Deep learning for basal cell carcinoma detection for reflectance confocal microscopy,” J. Invest. Dermatol., vol. 142, no. 1, pp. 97–103, 2022. doi: 10.1016/j.jid.2021.06.015.
16. J. Zhang et al., “Accuracy of Raman spectroscopy for differentiating skin cancer from normal tissue,” Medicine (Baltimore), vol. 97, no. 34, e12022, 2018. doi: 10.1097/MD.0000000000012022.
17. C. Delrue et al., “From vibrations to visions: Raman spectroscopy's impact on skin cancer diagnostics,” J. Clin. Med., vol. 12, no. 23, p. 7428, 2023. doi: 10.3390/jcm12237428.
18. L. Silveira Jr. et al., “Discriminating model for diagnosis of basal cell carcinoma and melanoma in vitro based on the Raman spectra of selected biochemicals,” J. Biomed. Opt., vol. 17, no. 7, p. 077003, 2012. doi: 10.1117/1.JBO.17.7.077003.
19. M. Gniadecka et al., “Melanoma diagnosis by Raman spectroscopy and neural networks: structure alterations in proteins and lipids in intact cancer tissue,” J. Invest. Dermatol., vol. 122, no. 2, pp. 443–449, 2004. doi: 10.1046/j.0022-202X.2004.22208.x.
20. J. Zhao et al., “Improving skin cancer detection by Raman spectroscopy using convolutional neural networks and data augmentation,” Front. Oncol., vol. 14, p. 1320220, 2024. doi: 10.3389/fonc.2024.1320220.
21. I. Jolliffe, “Principal component analysis,” in International Encyclopedia of Statistical Science, M. Lovric, Ed. Berlin, Heidelberg: Springer, 2011. doi: 10.1007/978-3-642-04898-2_455.
22. M. Greenacre et al., “Principal component analysis,” Nat. Rev. Methods Primers, vol. 2, no. 1, p. 100, 2022. doi: 10.1038/s43586-022-00184-w.
23. B. Bodanese et al., “Differentiating normal and basal cell carcinoma human skin by Raman spectroscopy: a comparison between principal components analysis and simplified biochemical models,” Photomed. Laser Surg., vol. 28, Suppl. 1, pp. S119–S127, 2010. doi: 10.1089/pho.2009.2565.
24. M. Gniadecka et al., “Diagnosis of basal cell carcinoma by Raman spectroscopy,” J. Raman Spectrosc., vol. 28, no. 2–3, pp. 125–129, 1997. doi: https://doi.org/10.1002/(SICI)1097-4555(199702)28:2/33.0.CO;2-%23